

# Study of Cs-Promoted, $\alpha$ -Alumina-Supported Silver, Ethylene Epoxidation Catalysts

## III. Characterization of Cs-Promoted and Nonpromoted Catalysts

David M. Minahan,\* Gar B. Hoflund,† William S. Epling,† and Dean W. Schoenfeld‡

\* Union Carbide Corporation, Technical Center/P.O. Box 8361, South Charleston, West Virginia 25303; and †Department of Chemical Engineering, and ‡Department of Chemistry, University of Florida, Gainesville, Florida 32611

Received September 9, 1996; revised January 27, 1997; accepted January 30, 1997

A nonpromoted Ag/ $\alpha$ -Al<sub>2</sub>O<sub>3</sub> catalyst and a Ag/ $\alpha$ -Al<sub>2</sub>O<sub>3</sub> catalyst promoted with 420 ppm Cs used for ethylene epoxidation were studied using scanning electron microscopy (SEM), ion scattering spectroscopy (ISS), Auger electron spectroscopy (AES), X-ray photoelectron spectroscopy (XPS), and secondary ion mass spectrometry (SIMS). SEM, ISS, XPS, and AES data indicate that the Cs-promoted catalyst consists of a thin film of Ag covering most of the support surface. Both a thin film and small Ag clusters exist on the nonpromoted catalyst, but the alumina is only partially covered. ISS and SIMS depth profiling data taken from the promoted catalyst indicate that most of the Cs lies beneath the surface although a small amount is present at the surface. The surface characterization data suggest that the Cs coats the support material during the preparation and acts as a binder between the Ag and the support resulting in a larger Ag coverage of the  $\alpha$ -alumina. Total oxidation of ethylene and ethylene oxide occur primarily on the alumina surface. The enhancement in selectivity toward ethylene epoxidation may result from the fact that Cs addition results in the thin Ag film covering the alumina. © 1997 Academic Press

### INTRODUCTION

The epoxidation of ethylene to ethylene oxide (EO) is an important industrial process because EO is a reaction intermediate in the formation of ethylene glycol and polyester fibers. Ethylene glycol is the primary constituent in antifreeze, and about 7.62 billion pounds were produced in 1995 (1). Ethylene oxide is most effectively produced by the partial oxidation of ethylene with air or oxygen over a silver-supported, low-surface-area,  $\alpha$ -alumina catalyst (2). Promoters, such as cesium or other alkali metals, are added to improve the selectivity of the reaction process (3–6). Without Cs the total conversion of ethylene is a little higher, but considerably more is burned to form CO<sub>2</sub> and H<sub>2</sub>O. The use of these promoted, Ag/ $\alpha$ -Al<sub>2</sub>O<sub>3</sub> catalysts for ethylene epoxidation results in industrial operating selectivities above 80% and single-pass conversions of 20 to 40%.

Complete oxidation of ethylene occurs over all other metal catalysts. Ag powder exhibits a low epoxidation rate which suggests that the Ag- $\alpha$ -Al<sub>2</sub>O<sub>3</sub> interaction or the manner in which the Ag is distributed over the  $\alpha$ -Al<sub>2</sub>O<sub>3</sub> plays an important role in this catalytic reaction. The  $\alpha$ -Al<sub>2</sub>O<sub>3</sub> must be low-surface area (<2 m<sup>2</sup>/g) and low acidity in order to avoid complete oxidation of ethylene and EO. Furthermore, large Ag particles are more effective in catalyzing this reaction than small Ag crystallites (7), and Ag metal loadings typically are high (>10 wt%). Therefore, Ag/ $\alpha$ -Al<sub>2</sub>O<sub>3</sub> catalysts are quite different than most oxide-supported metal catalysts in that they have high metal loading, large metal particles, low surface area and low acidity.

Many epoxidation reaction studies over Ag-containing catalysts and model studies of the interaction of oxygen with silver surfaces have been performed. An excellent review of these studies has been published by Van Santen and Kuipers (6). Only a few surface characterization studies, however, have been carried out on industrial-type epoxidation catalysts (8–11). This study is the third part of a series which examines the preparation, characterization, and catalytic behavior of a Cs-promoted, Ag/ $\alpha$ -Al<sub>2</sub>O<sub>3</sub> catalyst which has demonstrated activity and selectivity in ethylene epoxidation (10). In the first part of this study (9), X-ray photoelectron spectroscopy (XPS), Auger electron spectroscopy (AES), ion scattering spectroscopy (ISS), and scanning electron microscopy (SEM) were used to characterize and compare the bare  $\alpha$ -alumina support and a Cs-promoted, Ag/ $\alpha$ -Al<sub>2</sub>O<sub>3</sub> catalyst. The effect of the reaction process on the surface as a function of catalyst age was examined in the second part of this study (10). Each characterization technique provides unique information concerning the catalyst surface region, and the combined results yield a better understanding of the catalytic chemistry. In the present paper the effects of the Cs promoter on the composition of the surface, chemical states in the near-surface region and the surface morphology of an ethylene epoxidation catalyst have been studied. In order to accomplish this study, XPS,

AES, ISS, and SEM and have been used to examine the differences between a Cs-promoted and a nonpromoted Ag/ $\alpha$ -Al<sub>2</sub>O<sub>3</sub> catalyst. Secondary ion mass spectrometry (SIMS) and ISS also were used to depth profile the Cs-promoted catalyst.

## EXPERIMENTAL

### Catalyst Preparation

The  $\alpha$ -alumina-supported Ag catalysts were prepared by an impregnation method based on a patent by Bhasin *et al.* (12) as described in the previous studies (9, 10). An 88 wt% lactic acid solution was heated to 75°C. In the formation of the Cs-promoted catalyst, a CsOH solution was added at this stage while stirring. The impregnating solution was allowed to drain from the alumina for 1 h in both cases, but it drained more rapidly off the solid when Cs is not present. After drying at 500°C the Cs-promoted catalyst contained 13.87 wt% Ag (420 ppm by weight Cs) and the nonpromoted catalyst contained 12.78 wt% Ag.

### Surface Characterization

The catalyst pellets were physically ground in order to perform the characterization studies, except in the SIMS experiments in which the pellet surface was analyzed. Grinding the catalyst and pressing the resulting powder into an Al cup exposes the catalytically active surface within the pores. This is the region of interest for the surface characterization studies. The Al cup containing the catalyst was entered into the ultrahigh vacuum chamber (base pressure of 10<sup>-11</sup> Torr). XPS, AES, and ISS data were collected using a double-pass cylindrical mirror analyzer (CMA) (Perkin-Elmer PHI Model 25-270AR). The experimental details have been provided previously (9, 10). The XPS binding energies (BE) were referenced by assignment of the Fermi level to a BE value of 0.0 eV and assignment of the primary Al 2*p* peak to the BE of Al in Al<sub>2</sub>O<sub>3</sub>. Differential charging influenced the XPS data as discussed below.

Depth profiles were obtained using both ISS and SIMS after completion of the other characterization studies. A 1-keV He<sup>+</sup> beam was used for the ISS depth profile with spectra taken at various time intervals. SIMS data were collected using a Perkin-Elmer spectrometer (PHI 6600) operated in quasi-static mode at the sample surface and in a fully dynamic mode for depth profiles below the surface layer. The oxygen duoplasmatron ion source was coupled with a charge-suppression electron flood gun. Peak switching of the RF quadrupole mass analyzer for selected ion monitoring was used for the depth profiles. A 35- $\mu$ m full width at half maximum beam at an angle of 30° off the surface plane was rastered over a 0.2-mm (or 0.5-mm) square surface area and the secondary ion counts/sec versus *m/z* ratio (Daltons) was recorded.

## RESULTS AND DISCUSSION

An SEM micrograph obtained from the nonpromoted Ag/ $\alpha$ -Al<sub>2</sub>O<sub>3</sub> catalyst is shown in Fig. 1a. Thin-film structures and small Ag crystallites are present on top of an underlying planar structure. SEM data obtained from the  $\alpha$ -alumina support (9) show the alumina to be crystalline with flat, planar surfaces exposed. This is the planar structure which is observable underneath the patchwork films and Ag crystallites in Fig. 1a. The SEM micrograph shown in Fig. 1b was obtained from the Cs-promoted catalyst. As demonstrated in the previous study (9), a thin Ag film covers the alumina surface. Although no small Ag clusters are evident, the film apparently is thicker in some regions than others based on variations in the EDS compositional data (9). This film agglomerates forming large Ag crystallites with aging in the reactor (10). In the presence of Cs, the Ag appears to wet the  $\alpha$ -Al<sub>2</sub>O<sub>3</sub> surface based on the high coverage and lack of crystallites with large contact angles. The differences between these two surfaces correlate with the fact that the lactic acid solution drains more slowly off the solid when Cs is present. The Cs also results in a larger Ag uptake (13.87 versus 12.78 wt% Ag). The additional 1.1 wt% Ag probably represents the thin film which is spread across the  $\alpha$ -Al<sub>2</sub>O<sub>3</sub>.

ISS spectra obtained from the nonpromoted and Cs-promoted catalysts are shown in Figs. 2a and 2b, respectively. ISS is a powerful surface characterization technique because it yields compositional information about the outermost atomic layer. The spectrum obtained from the nonpromoted catalyst contains features due to Ag, Al, and O as well as C, Ca, and Ni contaminants. The spectrum taken from the promoted catalyst has features due to Ag and O as well as Na, S, Cl, Ca, and Ni contamination. Some Al may be present, but a well-defined Al peak is not apparent. The O and Al features are smaller with respect to the Ag peak compared to the spectrum obtained from the nonpromoted catalyst, and much of the O is associated with the Ag film (13). A previous study has shown that the ISS sensitivity for Ag is about 20 times greater than that for O (13). Both the SEM and the ISS data therefore indicate that the Ag covers considerably more of the support on the Cs-promoted catalyst. AES data obtained from the nonpromoted and promoted catalysts are presented in Figs. 3a and 3b, respectively. The predominant peaks in these spectra are due to Ag, O, and Al, and small peaks due to Si and Cl also are present. In these spectra the Ag-to-O and Ag-to-Al peak-height ratios are much larger in the spectrum obtained from the Cs-promoted catalyst. Since the difference in the amounts of Ag on these surfaces is small, the large differences in the peak-height ratios are due to a matrix effect: i.e., differences in the spatial distribution of the elements in the near-surface region. These Auger data support the assertion that the Ag forms a film covering the

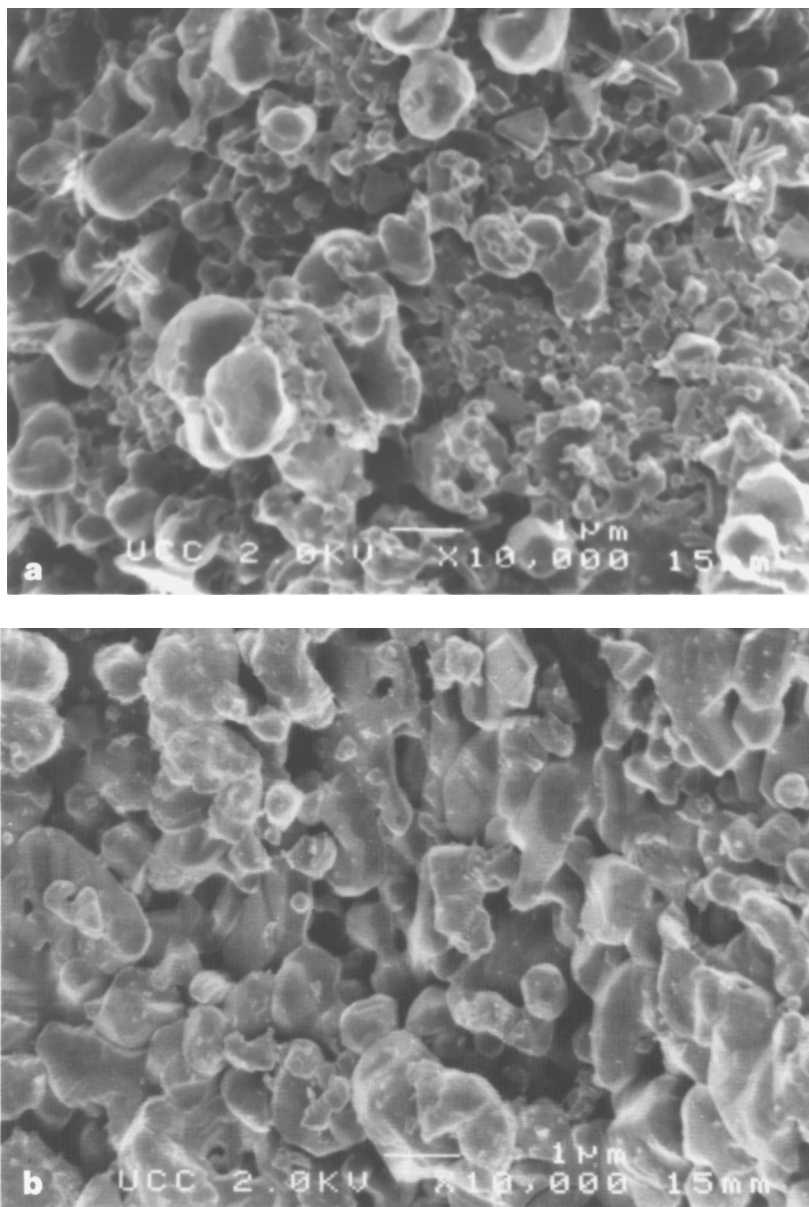


FIG. 1. SEM micrographs obtained from (a) the nonpromoted and (b) the Cs-promoted  $\text{Ag}/\alpha\text{-Al}_2\text{O}_3$  catalysts.

$\alpha\text{-Al}_2\text{O}_3$  when Cs is present and that a considerable amount of  $\alpha\text{-Al}_2\text{O}_3$  is exposed when Cs is not present. Based upon the assumption of surface homogeneity and published sensitivity factors (14), the near-surface region of the promoted catalyst contains about 3.3 times as much Ag as the nonpromoted catalyst. This is not the case indicating that use of the homogeneous assumption is incorrect and leads to a serious error. The comparison of SEM, ISS, and AES data provide a way of understanding the matrix effect and of taking it into account in a qualitative manner.

An XPS survey spectrum taken from the nonpromoted  $\text{Ag}/\alpha\text{-Al}_2\text{O}_3$  catalyst is shown in Fig. 4a. Auger (A) and

photoemission peaks due to Ag, Al, O, and C are apparent. A distinct C 1s peak is not observed in the corresponding Auger spectrum shown in Fig. 3a because C has a low sensitivity in AES. Therefore, it is overshadowed by the Ag feature at 275 eV. Also, XPS probes more deeply for C than AES due to mean-free-path differences so some of the C contamination contributing to Fig. 4a may lie beneath the Auger sampling depth. The survey spectrum obtained from the Cs-promoted catalyst is shown in Fig. 4b. Consistent with the Auger spectra shown in Fig. 3, both the Ag-to-O and the Ag-to-Al peak-height ratios are much larger than those for the nonpromoted catalyst. Since the near-surface

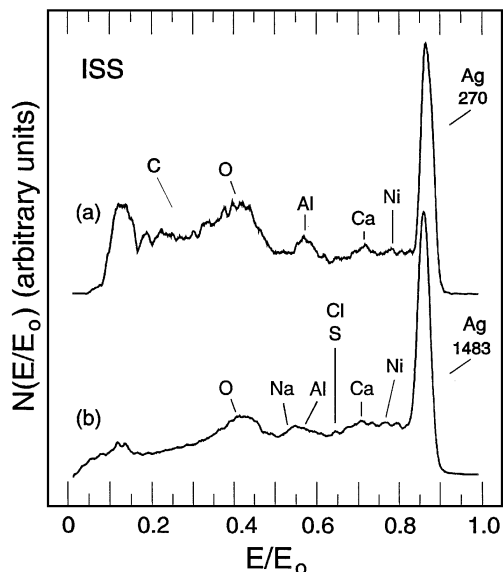


FIG. 2. ISS spectra obtained from (a) the nonpromoted and (b) the Cs-promoted  $\text{Ag}/\alpha\text{-Al}_2\text{O}_3$  catalysts. The maximum numbers of counts are listed by the Ag peaks.

compositions are similar, the peak-height ratios again are dominated by the matrix effect which is observed directly in the SEM micrographs. This implies that the homogeneous assumption cannot be used to quantify the XPS data for the same reasons discussed above in conjunction with the Auger data.

The high-resolution, XPS Ag 3d spectra obtained from the nonpromoted and Cs-promoted catalysts are shown in Figs. 5a and 5b, respectively, and the corresponding O 1s,

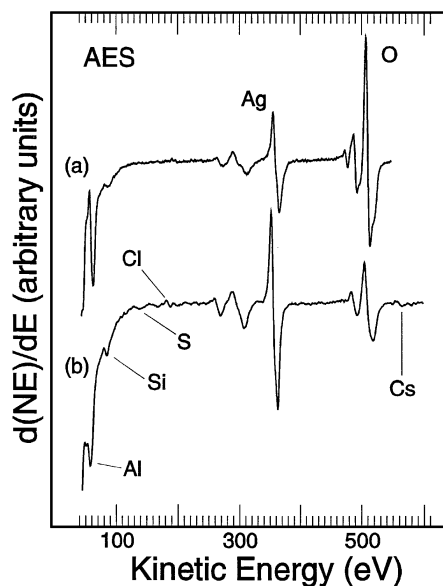


FIG. 3. AES spectra obtained from (a) the nonpromoted and (b) the Cs-promoted  $\text{Ag}/\alpha\text{-Al}_2\text{O}_3$  catalysts.

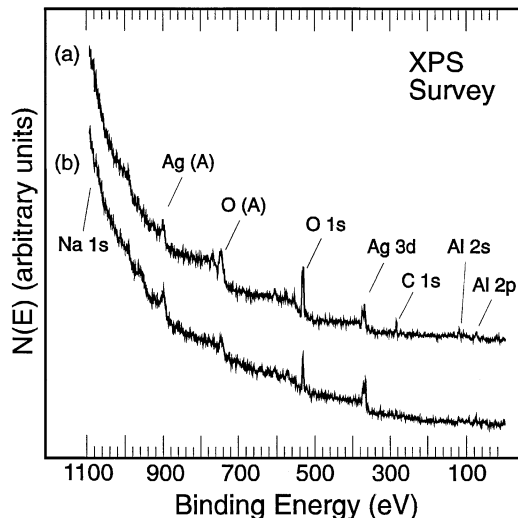


FIG. 4. XPS survey spectra obtained from (a) the nonpromoted and (b) the Cs-promoted  $\text{Ag}/\alpha\text{-Al}_2\text{O}_3$  catalysts.

Al 2p, Na 1s, and C 1s features are shown in Figs. 6a and 6b. Two distinct sets of Ag 3d, O 1s, Al 2p, and C 1s peaks are apparent in these spectra indicating that differential charging occurred during collection of these spectra. Interpretation of XPS data influenced by differential charging is difficult and usually speculative. An attempt is made here to interpret these spectra. The interpretation is based on the fact that different regions of a sample charge by different amounts. This fact makes differential charging useful in understanding complex morphologies such as this. The O 1s and Al 2p peaks in Fig. 6 are labeled 1 and 2. The O and Al features labeled 1 originate from  $\text{Al}_2\text{O}_3$  covered by the Ag film, and the O and Al features labeled 2 originate

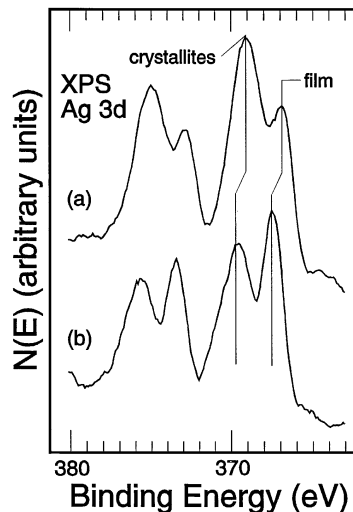


FIG. 5. XPS Ag 3d spectra obtained from (a) the nonpromoted and (b) the Cs-promoted  $\text{Ag}/\alpha\text{-Al}_2\text{O}_3$  catalysts.

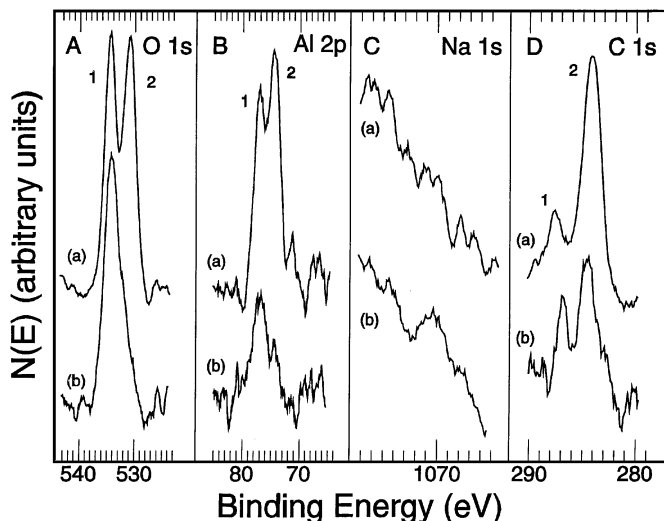


FIG. 6. XPS (A) O 1s, (B) Al 2p, (C) Na 1s, and (D) C 1s spectra obtained from (a) the nonpromoted and (b) the Cs-promoted  $\text{Ag}/\alpha\text{-Al}_2\text{O}_3$  catalysts.

from  $\text{Al}_2\text{O}_3$  which is exposed. These assignments are consistent with the facts that only a small amount of  $\text{Al}_2\text{O}_3$  is exposed on the Cs-containing catalysts while a large amount of  $\text{Al}_2\text{O}_3$  is exposed on the nonpromoted catalyst. Furthermore, the O 1s and Al 2p peak sizes are smaller in the spectra obtained from the Cs-promoted catalyst as shown in Fig. 4. The two sets of Ag 3d features in the spectra shown in Fig. 5 are interpreted as arising from the thin Ag film and from larger Ag crystallites. The ratio of Ag contributing to the film to Ag contributing to crystallites is larger for the Cs-promoted catalyst. This is consistent with the SEM, ISS, AES, and XPS survey data. Differential charging makes it difficult to obtain chemical-state information. For both catalysts the crystallite peak is broader than the thin-film peak indicating that multiple Ag states are present as discussed previously for the Cs-containing catalyst (9). In that study the peaks were shifted to perform a chemical-state analysis, and it was determined that the crystallites contain Ag metal, AgO, and  $\text{Ag}_2\text{O}$ . In this study the Ag features are shifted by the same amounts of the other features. The Ag film features are associated with the lower-BE O 1s and Al 2p features. They have different BEs but are characteristic of an oxide. On the nonpromoted catalyst the Ag film is bonded to alumina while on the Cs-promoted catalyst the Ag is bonded to the alumina through Cs. This chemical difference most likely is responsible for the difference in BEs of the Ag film peak. The peaks assigned as crystallite (or thick regions of the film) are due to Ag regions which are small spatially compared to the thin-film region so they do not affect the O 1s or Al 2p peaks.

Although Na is a binder material in the alumina support, the Na 1s XPS spectra taken from the nonpromoted

and promoted catalysts shown in part C of Figs. 6a and 6b exhibit no Na feature and a very small Na feature respectively. The bare alumina support material contains a significant amount of Na in the near-surface region according to XPS (Figs. 4a and 6Da of Ref. 9). Apparently, most of the Na migrates beneath the probing depth of XPS during the preparation of these catalysts or is removed from the surface. The C 1s XPS spectrum taken from the nonpromoted catalyst is shown in Fig. 6a, part D, and that obtained from the promoted catalyst is shown in Fig. 6b. These spectra exhibit two peaks (1 and 2). The relative peak sizes are quite different as can be seen in the survey spectra shown in Fig. 4. The C 1s peak obtained from the nonpromoted catalyst is very large and similar to the C 1s feature obtained from the bare alumina support (9). Feature 1 is assigned as due to the presence of carbonates or bicarbonates adsorbed on the alumina or Ag (15, 16), and feature 2 is assigned as due to hydrocarbons. The C 1s peak obtained from the Cs-promoted sample is so small that it is not visible in the corresponding survey spectrum. Features 1 and 2 have a different BE difference than those in Fig. 6(a) and are assigned as due to hydrocarbons adsorbed on Ag and exposed alumina, respectively. The difference in BE is a result of charging.

The presence of the Cs in the catalyst induces a greater coverage of Ag over the support and a greater Ag/Al interfacial area. Thus far, however, no Cs has been observable in the XPS spectra presented. The XPS spectra of the Cs 3d/BE region obtained from the nonpromoted and Cs-promoted catalysts are shown in Figs. 7a and 7b, respectively. No Cs is observable in either spectrum. This indicates either that the amount of Cs in the region probed is below the detection

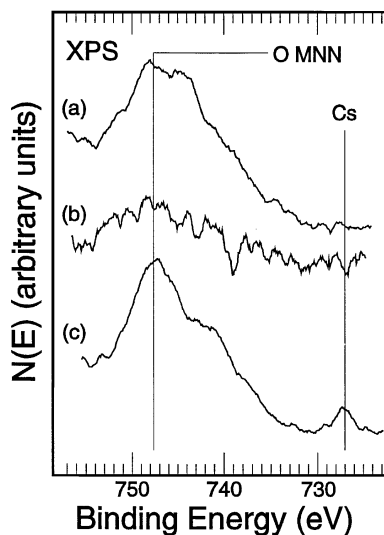


FIG. 7. XPS Cs 3d spectra obtained from (a) the nonpromoted, (b) the fresh, Cs-promoted,  $\text{Ag}/\alpha\text{-Al}_2\text{O}_3$  catalyst, and (c) the aged, Cs-promoted,  $\text{Ag}/\alpha\text{-Al}_2\text{O}_3$  catalyst.

level or that most of the Cs lies beneath the region examined by XPS. An XPS spectrum taken from a Cs-promoted catalyst after it has been run under reaction conditions for 24 days is shown in Fig. 7c. The Cs feature is now apparent because the Ag has sintered, forming large clusters which leaves the alumina support exposed (10). During the reaction process, either the Cs migrates to the near-surface region or it lies between the Ag and the support and becomes exposed as the Ag agglomerates exposing the support. The chemical state of the Cs remains unclear. Although interactions between the Ag and Cs and the Al and Cs occur, BE values have not been published for such species. A model study has begun which may provide information about the chemical state of the Cs in these catalysts.

An expanded ISS Ag/Cs spectrum taken from the fresh Cs-promoted catalyst is shown in Fig. 8a. A subtle shoulder is apparent on the Ag feature at an  $E/E_0$  value of 0.89 which corresponds to Cs. After sputtering the sample with a 1-keV  $\text{He}^+$  beam, the intensity of this feature decreases as shown in Fig. 8b. The spectrum shown in Fig. 8c was taken after 6 h of sputtering at a very low rate. The Cs feature is apparent as a distinct shoulder on the Ag peak. These data indicate that a small amount of Cs is located in the outermost surface layer but that most of the Cs lies beneath the Ag layer which is slowly sputtered off. These data are consistent with the assertion that most of the Cs lies beneath the Ag possibly acting as a binder between the Ag and  $\alpha\text{-Al}_2\text{O}_3$  support. Unpublished results of the adsorption of CsOH onto the  $\alpha\text{-alumina}$  support show that the  $\alpha\text{-alumina}$  adsorbs CsOH readily onto the surface and that the CsOH nearly covers

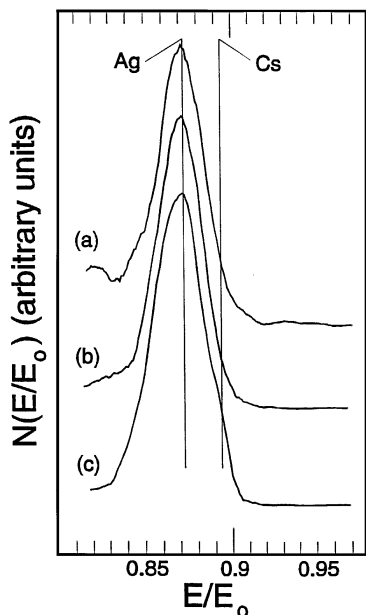


FIG. 8. ISS spectra obtained from the Cs-promoted Ag/ $\alpha\text{-Al}_2\text{O}_3$  catalyst after sputtering with a 1-keV  $\text{He}^+$  beam for (a) 0 min, (b) 5 h, and (c) 6 h.

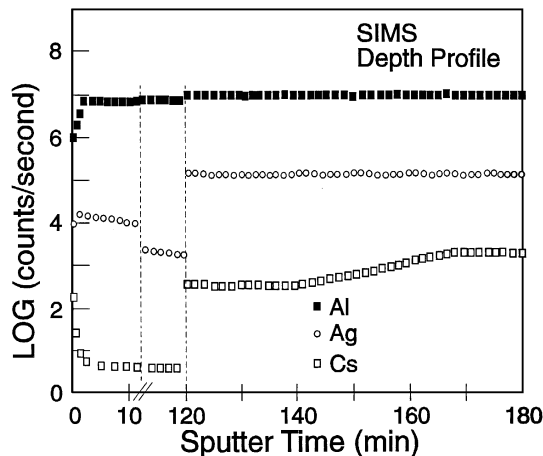


FIG. 9. SIMS depth profile obtained from the Cs-promoted Ag/ $\alpha\text{-Al}_2\text{O}_3$  catalyst.

the support material completely. A separate depth profile obtained using SIMS is shown in Fig. 9. The near-surface region was measured with the instrument in a quasi-static mode. The 2-keV oxygen-ion beam current was 60 nA with a 0.5-mm square raster area for 120 min. The raster was decreased to a  $0.2 \times 0.2$ -mm area to obtain a 6-fold increase in the primary ion current density and sputtering rate. This was coupled with a 16-fold increase in the  $\text{O}^+$  beam current to  $1 \mu\text{A}$  and a concurrent increase in the beam energy to 5 keV. The Cs concentration shown in Fig. 9 quickly decreases with sputtering while both the Ag and Al signals increase. This Cs is associated with the outermost surface layers of the Ag film. After approximately 10 min of sputtering, the Cs concentration achieves a constant value. After 2 h of sputtering, the primary beam flux was increased approximately by a factor of 50. The Cs concentration then begins to increase after sputtering for 20 min at this setting. These results are in agreement with the ISS data presented above in that there is a small amount of Cs at the catalyst surface and that more Cs is present between the Ag and the  $\text{Al}_2\text{O}_3$ , acting as a binder between the Ag and support.

The catalytic behavior of the nonpromoted catalyst has not been measured in this study. The presence of Cs is known to improve the selectivity of Ag/ $\alpha\text{-Al}_2\text{O}_3$  catalysts for ethylene epoxidation (6), and the data presented in this study provide insight as to how the Cs functions. The complete oxidation of ethylene and EO to  $\text{CO}_2$  and  $\text{H}_2\text{O}$  occurs primarily on the  $\alpha\text{-Al}_2\text{O}_3$  surface. This is the reason why low-area supports are used for this reaction. Since more of the  $\alpha\text{-Al}_2\text{O}_3$  surface is covered by Ag, the complete oxidation reaction is suppressed resulting in improved selectivity. The electronic influence, if any, on the catalytic behavior is not understood. Cs is present both at the Ag-alumina interface and at the Ag surface in smaller quantities. The two forms of Cs may differ chemically and their electronic influence may differ accordingly.

## SUMMARY

Nonpromoted Ag/ $\alpha$ -Al<sub>2</sub>O<sub>3</sub> and Cs-promoted Ag/ $\alpha$ -Al<sub>2</sub>O<sub>3</sub>, ethylene epoxidation catalysts were examined using SEM, ISS, AES, and XPS. SEM micrographs show that the nonpromoted catalyst consists of small Ag clusters and a film of Ag while the Cs-promoted catalyst consists of a Ag film which covers most of the  $\alpha$ -Al<sub>2</sub>O<sub>3</sub>. ISS and AES data indicate that less Al<sub>2</sub>O<sub>3</sub> is observable on the Cs-promoted catalyst surface due to a greater Ag coverage of the support. Ca and Ni contaminants and some Na also are present in the outermost surface layer according to ISS. More C contamination is apparent on the nonpromoted catalyst which is associated with the exposed support material. SIMS and ISS data obtained from the Cs-promoted sample show that a small amount of the Cs promotor is observed at the surface but that most is located between the Ag film and the Al<sub>2</sub>O<sub>3</sub> support. It acts as a binder between the two and probably affects the electronic structure of the Ag/Al<sub>2</sub>O<sub>3</sub> interface.

## ACKNOWLEDGMENTS

Financial support for this research was provided by the National Science Foundation through Grant CTS-9122575. The scanning electron micrographs were obtained by Phil Tate.

## REFERENCES

1. *Chem. Eng. News* **74**, 41 (1996).
2. Lefort, T. E., (to Societe Francaise de Catalyse Generalisee), French Patent 729,952, March 27, 1931, and subsequent additions.
3. Nielsen, R. P., and LaRochelle, J. H., U.S. Patent 3,962,136 (1976) and U.S. Patent 4,012,425 (1977).
4. Berty, J. M., in "Applied Industrial Catalysis" edited by (B. E. Leach, Ed.), Vol. 1, p. 207. Academic Press, New York, 1983-1984.
5. Satterfield, C. N., "Heterogeneous Catalysis in Industrial Practice," 2nd ed. McGraw-Hill, New York, 1991.
6. Van Santen, R. A., and Kuipers, H. P. C. E., *Adv. Catal.* **35**, 265 (1987).
7. Goncharova, S. N., Paukshtis, E. A., and Bal'zhinimaev, B. S., *Appl. Catal. A* **126**, 67 (1995).
8. Ormerod, R. M., Peat, K. L., Wytenburg, W. J., and Lambert, R. M., *Surf. Sci.* **269/270**, 506 (1992).
9. Minahan, D. M., and Hoflund, G. B., *J. Catal.* **158**, 109 (1996).
10. Hoflund, G. B., and Minahan, D. M., *J. Catal.* **162**, 48 (1996).
11. Hoflund, G. B., and Minahan, D. M., *Nucl. Instrum. Meth. Phys. Res. B* **118**, 517 (1996).
12. Bhasin, M. M., Ellgen, P. C., and Hendrix, C. D., U.S. Patent 4,916,243 (1990).
13. Davidson, M. R., Hoflund, G. B., and Outlaw, R. A., *J. Vac. Sci. Technol. A* **9**, 1344 (1991).
14. Davis, L. E., Macdonald, N. C., Palmberg, P. W., Riach, G. E., and Weber, R. E., "Handbook of Auger Electron Spectroscopy." Physical Electronics Industries, Eden Prairie, MN, 1976.
15. Weaver, J. F., and Hoflund, G. B., *J. Phys. Chem.* **98**, 8519 (1994).
16. Weaver, J. F., and Hoflund, G. B., *Chem. Mater.* **6**, 1693 (1994).